IEEE Access
Multidisciplinary ⋮ Rapid Review ⋮ Open Access Journal

Received 6 November 2023, accepted 21 November 2023, date of publication 22 December 2023,
date of current version 28 December 2023.

Digital Object Identifier 10.1109/ACCESS.2023.3346034

RESEARCH ARTICLE

Joint Estimation Algorithm of Target State and Measurement Bias for Doppler Sensor

GUOQIANG SUN[1], TAO YAN[1,2], ZIXIONG YANG[1], AND WENBO WU[1]
[1]Faculty of Electronic and Information Engineering, School of Automation Science and Engineering, Xi'an Jiaotong University, Xi'an 710049, China
[2]Ministry of Education Key Laboratory for Intelligent Networks and Network Security, Xi'an Jiaotong University, Xi'an 710049, China

Corresponding author: Tao Yan (yantao@xjtu.edu.cn)

This work was supported in part by the Natural Science Foundation of Shaanxi Province under Grant 2021JM-021.

ABSTRACT In recent years, Doppler-only sensors have demonstrated an excellent estimation performance for target tracking. Most of the existing tracking algorithms that utilize Doppler sensors rely on the assumption that sensors capture only measurement errors, disregarding measurement biases. However, in many practical situations, there can be significant measurement biases, which can severely compromise the performance of target state estimation. Recognizing this issue, the study proposes a new joint estimation algorithm that is exclusively reliant on Doppler-only sensors. The proposed algorithm not only provides the estimated results of the target state, but also the measurement bias of the Doppler sensor in use. The approach unfolds in two stages: the first stage is to estimate the target state without considering the measurement bias; the second is to perform bias compensation using the least squares method, and the target state and measurement bias are jointly estimated by linearization of the measurement equation. To validate the efficacy of this method, we analyzed the Cramer-Rao lower bound (CRLB) for measurement bias estimation and designed simulations under both static and moving sensor scenarios to assess its performance. The results indicate that the proposed algorithm can effectively estimate the target state, outperforming Kalman filter (KF) in both the moving and static sensor scenario. The root mean square error (RMSE) of the bias estimation can approach the CRLB.

INDEX TERMS Target tracking, Doppler sensor, measurement bias, space registration.

I. INTRODUCTION

The Doppler radar, characterized as a pulse mechanism radar, leverages the Doppler effect to estimate the state of a moving target. By employing spectrum separation technology, Doppler radar can effectively suppress various background clutter, and serve a pivotal role in fields such as meteorological detection, missile guidance, and airborne early warning [1]. The Doppler radar emits electromagnetic wave signals into the external environment and receives reflected echoes. Through analysis and processing of these echoes, information regarding the state of the target can be extracted. Conventional radar detection can only determine the distance between the radar itself and the target, as well as the azimuth and elevation angles. In contrast, Doppler radar processes the frequency of the reflected signals to gauge the Doppler frequency shift, enabling the calculation of the radial velocity information of the target. Doppler-only sensors can detect and locate targets under all weather conditions, even in complex and fluctuating battlefield environments. They hold a crucial position in the national defense infrastructure and serve as indispensable equipment in modern defense systems [2].

Target detection and state estimation constitute are vital components of radar-signal processing [3]. In the estimation of the target state, measurements are gathered from deployed sensors and subsequently employed to deduce the true state of the target using optimization or filtering techniques [4]. A variety of measurements are provided by different types of sensors. For MIMO (Multiple Input Multiple Output) radar systems, TOA (Time-of-Arrival) measurements were mentioned in [5]. The TOA can achieve higher positioning accuracy because it reduces the influence of low azimuth angle accuracy on localization accuracy. For medical image

The associate editor coordinating the review of this manuscript and approving it for publication was Xiwang Dong.

observation, DOA (Direction-of-Arrival) measurement was mentioned in [6] and [7]. Merging the DOA and TOA with filters can significantly improve the target localization performance. The Doppler frequency shift is a commonly used measurement for Doppler radar, which is simple to evaluate and has been widely used [8], [9]. Target estimation using Doppler-only shift measurement is an ancient problem researched in various studies [10], [11]. The Doppler sensor performs state estimation using a single-channel antenna. Therefore, unlike TOA and DOA sensors, it does not require the process of stringent data synchronization. Meanwhile, the measurement model of the Doppler sensor exhibits greater non-linearity, compared with TOA and DOA measurements [21].

Even with fully calibrated Doppler sensors, numerous challenges persist in target state estimation solely through Doppler sensors. This can be explained as follows. Firstly, the target state and the measurement share a high degree of non-linear relationship, which complicates the task of finding the optimal solution for the target state [13]. Secondly, factors, including observability [14] and sensor deployment [17], significantly affect the performance of target state estimation. In recent years, several studies have been conducted on Doppler-only radar systems [15], [16]. In practical scenarios, the presence of measurement bias in Doppler-only sensors can lead to a dramatic decrease in performance, or even divergence in typical target state estimation algorithms.

A feasible approach to calibrating Doppler measurement bias is through extended dimension filtering, where the dimensionality of the state variables is increased to jointly estimate both the target state and measurement bias simultaneously [18]. The estimation of the measurement bias is utilized to enhance the estimation of the target state, with the augmented vector derived through the method of maximum likelihood estimation. Existing approaches include linearization methods based on Taylor series expansion [19] and methods utilizing trajectory generator to estimate the initial measurement bias [20]. Convenient methods for simultaneously estimating the target state and measurement bias remain to be investigated.

In summary, two important problems need to be solved for Doppler-only sensor state estimation: One is to find an appropriate measurement model, i.e. Doppler shift, to characterize target motion; The other is to jointly estimate target state and measurement bias. Hence, this paper focuses on the issue of joint target state estimation and sensor registration for Doppler-only sensors. The proposed algorithm in this paper involves two main steps. Firstly, assuming that the Doppler sensor has no measurement bias, an initial estimation of the target states is conducted. Then bias compensation is executed based on the obtained initial estimation. Secondly, a linear-least squares estimation is established. The analytical solution for this estimation can be effectively determined through analysis and deduction. At the same time, the Cramer-Rao Lower bound (CRLB) of collaborative target tracking using multiple Doppler sensors is derived to compare the estimation precision. Finally, the effectiveness of the algorithm is verified through simulations in both static and moving sensor scenarios.

The main contribution of this paper is to propose a novel algorithm that can jointly estimate target state and measurement bias for Doppler-only sensors in a satisfying accuracy. The subsequent sections of this paper are organized as follows. Section II describes the mathematical foundations of the target motion model and Doppler sensor measurement model. The preliminary content of target state estimation is also introduced. In Section III, a new joint estimation algorithm for the target state and measurement bias is proposed, and the derivation of the Cramer-Rao lower bound is illustrated. Simulations of different scenarios are presented in Section IV to verify the performances of the proposed joint estimation algorithm. Finally, conclusions are drawn in Section V.

II. BACKGROUNDS

In this section, we first delineate the motion models of the targets and the frequency measurement models pertinent to the Doppler sensors in detail. Subsequently, we introduce algorithms for target state estimation based on Doppler sensors. This establishes the mathematical foundations for the proposed algorithm.

A. TARGET MOTION MODEL

This study focuses on the problem of tracking a given non-cooperative target using Doppler sensors. Common target motion models include the constant velocity model, constant acceleration model, Singer acceleration model, and constant turn rate model. In this study, it is assumed that the target's motion model can be approximated by the constant velocity (CV) motion model, thereby deriving the following target state transition equations.

$$\boldsymbol{x}_{k+1} = \boldsymbol{F}\boldsymbol{x}_k + \boldsymbol{G}\boldsymbol{w}_k, \tag{1}$$

where k denotes time, $\boldsymbol{x}_k$ is the target state vector at time k, $\boldsymbol{F}$ is the system state transition matrix, $\boldsymbol{w}_k$ is the process noise, and $\boldsymbol{G}$ is the noise matrix. The process noise $\boldsymbol{w}_k$ is a zero-mean white noise process, encompassing random variations in velocity in both the x and y directions, with the covariance matrix denoted as $\boldsymbol{Q}$.

The target state at time k is defined as $\boldsymbol{x}_k \triangleq [x_k, y_k, \dot{x}_k, \dot{y}_k]^{\mathrm{T}}$, where x_k, y_k and $\dot{x}_k, \dot{y}_k$ represent the position and velocity of the target in the Cartesian coordinate system, respectively. Under a two-dimensional constant velocity motion, the definitions of the state transition matrix $\boldsymbol{F}$, noise transition matrix $\boldsymbol{G}$, and covariance $\boldsymbol{Q}$ are as follows.

$$\boldsymbol{F} = \begin{bmatrix} 1 & 0 & T & 0 \\ 0 & 1 & 0 & T \\ 0 & 0 & 1 & 0 \\ 0 & 0 & 0 & 1 \end{bmatrix}, \tag{2}$$

$$\boldsymbol{G} = \begin{bmatrix} \frac{T^2}{2} & 0 \\ \frac{T^2}{2} & 0 \\ 0 & T \\ 0 & T \end{bmatrix}, \tag{3}$$

$$\boldsymbol{Q} = \begin{bmatrix} \sigma_\alpha & 0 \\ 0 & \sigma_\beta \end{bmatrix}, \tag{4}$$

where T represents the sampling period, σ_α and σ_β represent the velocity variances along the x and y directions, respectively. It is assumed that all Doppler sensors are synchronized in time.

Furthermore, for convenience, we define the position vector of the target as $\boldsymbol{p}_k \triangleq [x_k, y_k]^{\mathrm{T}}$ and the velocity vector as $\boldsymbol{v}_k \triangleq [\dot{x}_k, \dot{y}_k]^{\mathrm{T}}$. $\boldsymbol{p}_k$ and $\boldsymbol{v}_k$ can be composed of the state vectors of the target. Clearly, $\boldsymbol{x}_k = [\boldsymbol{p}_k^{\mathrm{T}}, \boldsymbol{v}_k^{\mathrm{T}}]^{\mathrm{T}}$.

B. DOPPLER SENSOR MEASUREMENT MODEL

This study is based on a multi-sensor environment, where M Doppler sensors are deployed in a two-dimensional space to estimate the target state. These sensors can be either static or moving.

Define $f_m'(\boldsymbol{x}_k)$ as the frequency of the signal from the target received by sensor $m \in \{1, \ldots, M\}$ at time k,

$$f_m'(\boldsymbol{x}_k) = f_t + f_m(\boldsymbol{x}_k) + f_{dm} + q_m(k), \tag{5}$$

where f is the target's emitting signal frequency, f_{dm} is the fixed bias caused by sensor system errors, and $q_m(k)$ represents the zero-mean Gaussian measurement noise. The $f_m(\boldsymbol{x}_k)$ represents the target Doppler frequency shift, which is obtained using the following formula according to the Doppler effect equation:

$$f_m(\boldsymbol{x}_k) = \frac{1}{\lambda}\left\{\frac{(\boldsymbol{p}_k - \boldsymbol{p}_m)^{\mathrm{T}}}{\|\boldsymbol{p}_k - \boldsymbol{p}_m\|}\right\}\boldsymbol{v}_k, \tag{6}$$

where λ is the signal wavelength, and $\boldsymbol{p}_m \triangleq [x_m, y_m]^{\mathrm{T}}$ is the known position of the Doppler sensor m, $\boldsymbol{p}_k$ and $\boldsymbol{v}_k$ are the target's position and velocity vectors, respectively.

Given that the target's emitting signal frequency, denoted as f_t, is a constant, the Doppler frequency shift caused by the target's motion is more worthy of study. Therefore, the measurement $z_m(k)$ from Doppler sensor m at time k is defined as the difference between the received signal frequency $f_m'(\boldsymbol{x}_k)$ and the target's emitting signal frequency f_t.

$$z_m(k) \triangleq f_m'(\boldsymbol{x}_k) - f_t = f_m(\boldsymbol{x}_k) + f_{dm} + q_m(k) \tag{7}$$

Clearly, for a perfectly calibrated Doppler sensor, $f_{dm} = 0$. Combining all the Doppler sensors, the Doppler frequency shift measurement vector is defined as $\boldsymbol{z}_k \triangleq [z_1(k), \ldots, z_M(k)]^{\mathrm{T}}$.

C. TSE USING DOPPLER SENSORS

In the scenarios where the sensors have no measurement bias (i.e., $f_{dm} = 0$), the target state estimation process can be simplified. This section briefly outlines the algorithm for target state estimation using Doppler sensors and establishes the foundation for the algorithm proposed in this paper. By multiplying (7) by λ, we obtain the measured range rate as follows.

$$\eta_m(k) = \lambda z_m(k) = \frac{(\boldsymbol{p}_k - \boldsymbol{p}_m)^{\mathrm{T}}}{\|\boldsymbol{p}_k - \boldsymbol{p}_m\|}\boldsymbol{v}_k + \lambda f_{dm} + \lambda q_m(k) \tag{8}$$

For the case involving M Doppler sensors, multiple formulas in (8) are stacked to yield the measured range rate vector, which can be denoted as $\boldsymbol{\eta}(k)$.

$$\boldsymbol{\eta}(k) = \boldsymbol{A}(\boldsymbol{p}_k)\boldsymbol{v}_k + \boldsymbol{q}_k, \tag{9}$$

where

$$\boldsymbol{\eta}_k = [\eta_1(k), \eta_2(k), \ldots, \eta_M(k)]^{\mathrm{T}}, \tag{10}$$

$$\boldsymbol{A}(\boldsymbol{p}_k) = \left[\frac{(\boldsymbol{p}_k - \boldsymbol{p}_1)}{\|\boldsymbol{p}_k - \boldsymbol{p}_1\|}, \ldots, \frac{(\boldsymbol{p}_k - \boldsymbol{p}_M)}{\|\boldsymbol{p}_k - \boldsymbol{p}_M\|}\right]^{\mathrm{T}}, \tag{11}$$

$$\boldsymbol{q}_k = [q_1(k), q_2(k), \ldots, q_M(k)]^{\mathrm{T}}, \tag{12}$$

the Gaussian vector $\boldsymbol{q}_k$ with mean 0 and variance $\boldsymbol{R} = \sigma^2\mathbf{I}$ is obtained.

In (9), the target states $\boldsymbol{p}_k$ and $\boldsymbol{v}_k$ served as the estimation parameters and can be solved with the least square method, requiring individual solutions for each parameter. The maximum likelihood function is expressed as follows.

$$\begin{aligned}&[\hat{\boldsymbol{p}}_k, \hat{\boldsymbol{v}}_k] \\ &= \arg\min_{\boldsymbol{p}_k, \boldsymbol{v}_k}\left[(\boldsymbol{\eta}_k - \boldsymbol{A}(\boldsymbol{p}_k)\boldsymbol{v}_k)^{\mathrm{T}}\boldsymbol{R}^{-1}(\boldsymbol{\eta}_k - \boldsymbol{A}(\boldsymbol{p}_k)\boldsymbol{v}_k)\right].\end{aligned} \tag{13}$$

The estimation problem above is solved as described in [22]. The following is a summary of the solution steps.

Firstly, the target position vector estimation is given by the following expression.

$$\hat{\boldsymbol{p}}_k = \arg\min_{\boldsymbol{p}_k} \boldsymbol{\eta}_k^{\mathrm{T}}\boldsymbol{P}_A(\boldsymbol{p}_k)\boldsymbol{\eta}_k, \tag{14}$$

$$\boldsymbol{P}_A(\boldsymbol{p}_k) = \mathbf{I} - \boldsymbol{A}(\boldsymbol{p}_k)\left(\boldsymbol{A}^{\mathrm{T}}(\boldsymbol{p}_k)\boldsymbol{A}(\boldsymbol{p}_k)\right)^{-1}\boldsymbol{A}^{\mathrm{T}}(\boldsymbol{p}_k). \tag{15}$$

Here, the first predicted value of $\hat{\boldsymbol{p}}_k$ can be evaluated through a grid search, followed by iterations through gradient-based optimization. This ensures that $\hat{\boldsymbol{p}}_k$ converges to the global optimal as much as possible.

Subsequently, the target velocity vector estimation can be given by the following equation.

$$\hat{\boldsymbol{v}}_k = \left(\boldsymbol{A}^{\mathrm{T}}(\hat{\boldsymbol{p}}_k)\boldsymbol{A}(\hat{\boldsymbol{p}}_k)\right)^{-1}\boldsymbol{A}^{\mathrm{T}}(\hat{\boldsymbol{p}}_k)\boldsymbol{\eta}_k. \tag{16}$$

III. METHODS

In this section, we describe the procedure for the joint estimation of the target state and measurement bias using a linear least squares problem formulation, under the scenario where the Doppler sensors have a fixed bias, represented by $f_{dm} \neq 0$ (for $m = 1, \ldots, M$). Furthermore, we derive the Cramer-Rao Lower bound (CRLB), a theoretical benchmark

that delineates the minimum possible variance for an unbiased estimator. This contributes to the evaluation of the effectiveness of the algorithm.

A. JOINT ESTIMATION ALGORITHM BASED ON TIME WINDOW

When there is a measurement bias f_{dm} present in the Doppler sensors, assuming that the measurement noise is much smaller than the measurement bias, the performance of the estimation method discussed in Section II.C deteriorates significantly, potentially leading to estimation failure. Therefore, further improvements are necessary.

Given that the least squares method requires the superposition of multiple equations to estimate the system parameters, this study considers collecting Doppler frequency shift measurements over L consecutive time steps. Assuming a consecutive time step of $k, \ldots, k+L-1$, the problem in this section is transformed into determining all the biases f_{dm} (for $m = 1, \ldots, M$) of the Doppler sensors given the Doppler measurements $z_k, \ldots, z_{k+L-1}$ (which include biases), while accurately estimating the target position vector $\boldsymbol{p}_k$ and velocity vector $\boldsymbol{v}_k$. According to (8), the Doppler measurements are translated into $\eta_k, \ldots, \eta_{k+L-1}$. For a duration of $t = 0, 1, \ldots, L-1$, assuming a constant velocity (CV) model for the target motion model, the following formula can be obtained.

$$\begin{aligned}\eta_m(k+t) &= \lambda z_m(k+t) \qquad (17)\\ &= \frac{\left(\boldsymbol{p}_k + tT\boldsymbol{v}_k - \boldsymbol{p}_m\right)^{\mathrm{T}}}{\left\|\boldsymbol{p}_k + tT\boldsymbol{v}_k - \boldsymbol{p}_m\right\|}\boldsymbol{v}_k + \lambda f_{dm} + \lambda \boldsymbol{q}_m(k+t),\end{aligned}$$

$$h_m\left(\boldsymbol{x}_k, t, T\right) \triangleq \frac{\left(\boldsymbol{p}_k + tT\boldsymbol{v}_k - \boldsymbol{p}_m\right)^{\mathrm{T}}}{\left\|\boldsymbol{p}_k + tT\boldsymbol{v}_k - \boldsymbol{p}_m\right\|}\boldsymbol{v}_k. \qquad (18)$$

The proposed Algorithm in this paper operates as follows. Initially, we employ the method outlined in Section II.C to directly obtain the initial estimations of $\hat{\boldsymbol{p}}_k$ and $\hat{\boldsymbol{v}}_k$ from $\boldsymbol{\eta}_k$. Given that f_{dm} is not zero, the estimations acquired are biased. The true state of the target is expressed as

$$\boldsymbol{p}_k = \hat{\boldsymbol{p}}_k + \tilde{\boldsymbol{p}}_k, \quad \boldsymbol{v}_k = \hat{\boldsymbol{v}}_k + \tilde{\boldsymbol{v}}_k, \qquad (19)$$

where $\tilde{\boldsymbol{p}}_k$ and $\tilde{\boldsymbol{v}}_k$ represent the biases induced by f_{dm} and measurement noise.

Given that $\hat{\boldsymbol{p}}_k$ and $\hat{\boldsymbol{v}}_k$ can be resolved from (14) and (16), we obtain the state estimate $\hat{\boldsymbol{x}}_k = \left[\hat{\boldsymbol{p}}_k^{\mathrm{T}}, \hat{\boldsymbol{v}}_{\boldsymbol{k}}^{\mathrm{T}}\right]^{\mathrm{T}}$ (with bias). Through linearization, the Doppler measurement $\eta_m(k+t)$ can be expressed as

$$\eta_m(k+t) \approx \hat{h}_m(k) + \boldsymbol{H}_m(k+t)\begin{bmatrix}\tilde{\boldsymbol{p}}_k\\ \tilde{\boldsymbol{v}}_k\end{bmatrix} + \lambda f_{dm} + \lambda \boldsymbol{q}_m(k+t), \qquad (20)$$

$$\hat{h}_m(k) = h_m\left(\hat{\boldsymbol{x}}_k, 0, T\right) \qquad (21)$$

where the Jacobian matrix $\boldsymbol{H}_m(k+t)$ is given by

$$\boldsymbol{H}_m(k+t) = \left.\frac{\partial h_m\left(\boldsymbol{x}_k, t, T\right)}{\partial \boldsymbol{x}_k}\right|_{\boldsymbol{x}_k = \left[\hat{\boldsymbol{p}}_k^{\mathrm{T}}, \hat{\boldsymbol{v}}_{\boldsymbol{k}}^{\mathrm{T}}\right]^{\mathrm{T}}} \qquad (22)$$

The Jacobian matrix can be partitioned into

$$\boldsymbol{H}_m(k+t) = \left[\boldsymbol{H}_m^{p\,\mathrm{T}}(k+t), \boldsymbol{H}_m^{v\,\mathrm{T}}(k+t)\right]^{\mathrm{T}}, \qquad (23)$$

where $\boldsymbol{H}_m^p(k+t)$ and $\boldsymbol{H}_m^v(k+t)$ are obtained as (24) and (25), shown at the bottom of the next page, where

$$\alpha_m(k+t) = \hat{\alpha}_k + tT\hat{\dot{\alpha}}_k - \alpha_m, \qquad (26)$$

$$\beta_m(k+t) = \hat{\beta}_k + tT\hat{\dot{\beta}}_k - \beta_m, \qquad (27)$$

$$\varphi_m\left(\boldsymbol{x}_k, t, T\right) = \left\|\hat{\boldsymbol{p}}_k + lT\hat{\boldsymbol{v}}_k - \boldsymbol{p}_m\right\|, \qquad (28)$$

where α and β represent the x and y directions, respectively. in the Cartesian coordinate system.

It is evident that (20) incorporates the three parameters that need to be estimated, namely $\tilde{\boldsymbol{p}}_k$, $\tilde{\boldsymbol{v}}_k$, and f_{dm}. Consequently, we can easily construct the input matrix $\boldsymbol{C}$, output matrix $\boldsymbol{d}$, and variable matrix $\boldsymbol{\theta}$ as follows. Finally, the least-squares equation is obtained as shown in equation (32).

$$\boldsymbol{C} = \begin{bmatrix}
\boldsymbol{H}_1^p(k+1) & \boldsymbol{H}_1^v(k+1) & 1\ 0\ \cdots\ 0\\
\vdots & \vdots & \vdots\ \vdots\ \vdots\ \vdots\\
\boldsymbol{H}_1^p(k+L-1) & \boldsymbol{H}_1^v(k+L-1) & 1\ 0\ \cdots\ 0\\
\boldsymbol{H}_2^p(k+1) & \boldsymbol{H}_2^v(k+1) & 0\ 1\ \cdots\ 0\\
\vdots & \vdots & \vdots\ \vdots\ \vdots\ \vdots\\
\boldsymbol{H}_2^p(k+L-1) & \boldsymbol{H}_2^v(k+L-1) & 0\ 1\ \cdots\ 0\\
\vdots & \vdots & \vdots\ \vdots\ \vdots\ \vdots\\
\boldsymbol{H}_M^p(k+1) & \boldsymbol{H}_M^p(k+1) & 0\ 0\ \cdots\ 1\\
\vdots & \vdots & \vdots\ \vdots\ \vdots\ \vdots\\
\boldsymbol{H}_M^p(k+L-1) & \boldsymbol{H}_M^p(k+L-1) & 0\ 0\ \cdots\ 1
\end{bmatrix}, \qquad (29)$$

$$\boldsymbol{d} = \begin{bmatrix}
\eta_1(k+1) - \hat{h}_1(k)\\
\vdots\\
\eta_M(k+1) - \hat{h}_M(k)\\
\eta_1(k+2) - \hat{h}_1(k)\\
\vdots\\
\eta_1(k+2) - \hat{h}_M(k)\\
\vdots\\
\eta_M(k+L-1) - \hat{h}_1(k)\\
\vdots\\
\eta_M(k+L-1) - \hat{h}_M(k)
\end{bmatrix}, \qquad (30)$$

$$\boldsymbol{\theta} \triangleq \left[\tilde{\boldsymbol{p}}_k, \tilde{\boldsymbol{v}}_k, \hat{f}_{d1}, \ldots, \hat{f}_{dM}\right], \qquad (31)$$

$$\boldsymbol{C}\boldsymbol{\theta} = \boldsymbol{d}. \qquad (32)$$

Therefore, the estimate of $\hat{\boldsymbol{\theta}}$ can be obtained from the solution of (31).

$$\hat{\boldsymbol{\theta}} = \left(\boldsymbol{C}^{\mathrm{T}}\boldsymbol{C}\right)^{-1}\boldsymbol{C}^{\mathrm{T}}\boldsymbol{d}. \qquad (33)$$

Up to this point, the final estimated values for the target position and velocity are $\hat{\boldsymbol{p}}_k + \hat{\boldsymbol{\theta}}(1:2)$ and $\hat{\boldsymbol{v}}_k + \hat{\boldsymbol{\theta}}(3:4)$,

respectively, whereas $\hat{f}_{d1}, \ldots, \hat{f}_{dM} = \hat{\boldsymbol{\theta}}(5 : M+4)$ represents the bias value of the Doppler sensor. Finally, Algorithm 1 summarizes the procedure proposed in Appendix B.

B. CRAMER-RAO LOWER BOUND

M Doppler sensors are deployed at appropriate locations, and a sufficient length of the time window L is employed. To derive the CRLB, the presence of measurement noise $\boldsymbol{q}$ is taken into consideration in (32). Moreover, the Jacobi matrix $\boldsymbol{C}$ is evaluated from the true target state, which is labeled $\tilde{\boldsymbol{C}}$ in this section. Therefore, (32) can be rewritten as follows,

$$\tilde{\boldsymbol{C}}\boldsymbol{\theta} + \lambda \boldsymbol{q} = \boldsymbol{d}, \tag{34}$$

$$\boldsymbol{q} = [q_1(k), \ldots, q_M(k), \ldots, q_1(k+L-1), \ldots, q_M(k+L-1)]^{\mathrm{T}}, \tag{35}$$

where $\boldsymbol{q}$ is stacked by the $q_m(k+t-1)$ for each time and sensor. Consequently, the following expression describes the constraint of the covariance matrix of unbiased estimator $\hat{\theta}$. The algorithm performs better when the variance of the estimator is closer to the Cramer-Rao bound.

$$\mathbb{E}\left\{(\hat{\boldsymbol{\theta}} - \boldsymbol{\theta})(\hat{\boldsymbol{\theta}} - \boldsymbol{\theta})^{\top}\right\} \geq \boldsymbol{J}^{-1}, \tag{36}$$

$$\boldsymbol{J} = \frac{\tilde{\boldsymbol{C}}^{\top}\tilde{\boldsymbol{C}}}{\lambda^2\sigma^2}, \tag{37}$$

where $\boldsymbol{J}$ denotes the Fisher Information Matrix (FIM).

IV. SIMULATION RESULTS

In this section, simulations in different scenarios are conducted to verify the proposed algorithm for the joint estimation of the target state and measurement bias. Static sensors are deployed in one scenario, and moving sensors are adopted in the alternative scenario. The simulation results are compared with the CRLB to verify the effectiveness of our algorithm.

A single target is assumed to move at a constant speed in a given two-dimensional(2D) area. Five Doppler sensors are deployed within this area to track the target. The parameters of the target movement are as follows. The process noise in x and y direction is denoted by $\sigma_\alpha = \sigma_\beta = 0.001\ \mathrm{m}^2/\mathrm{s}^2$, the sampling period is $T = 0.01$ s, and the target emitting signal frequency is 310 MHz. The standard deviation of the measurement noise is denoted by $\sigma = 2$ Hz. The initial state of the target is $x_0 = [-100\ \mathrm{m}, -100\ \mathrm{m}, 210\mathrm{m/s}, 210\ \mathrm{m/s}]$. The Doppler sensors bias vector is configured as $f_d = [40\ \mathrm{Hz}, -30\ \mathrm{Hz}, 40\ \mathrm{Hz}, -50\ \mathrm{Hz}, 20\ \mathrm{Hz}]$.

By using different window lengths L to evaluate the performance of the measurement bias. The following expression defines the estimation error of measurement bias.

$$\tilde{f}_{dm} = \left| f_{dm} - \hat{f}_{dm} \right|, m = 1, \ldots, M. \tag{38}$$

where $\tilde{f}_{dm}$ represents the estimation error of measurement bias, f_{dm} denotes the true value of the measurement bias, and $\hat{f}_{dm}$ denotes the estimated value of the measurement bias.

By using different times of estimation errors to evaluate the performance of the target state estimation, we consider the estimation errors, including the target position $error_p$ and target velocity $error_v$ at the initial time of the measurement window. The evaluations of $error_p$ and $error_v$ are as follows.

$$error_p = \sqrt{(\boldsymbol{p} - \hat{\boldsymbol{p}})^{\mathrm{T}}(\boldsymbol{p} - \hat{\boldsymbol{p}})}, \tag{39}$$

$$error_v = \sqrt{(\boldsymbol{v} - \hat{\boldsymbol{v}})^{\mathrm{T}}(\boldsymbol{v} - \hat{\boldsymbol{v}})}, \tag{40}$$

$$\boldsymbol{H}_m^p(k+t) = \left[\frac{\left(\varphi_m^2(\hat{\boldsymbol{x}}(k), t, T) - \alpha_m^2(k+t)\right)\hat{\alpha}(k) + \alpha(k+t)\beta_m(k+t)\hat{\beta}(k)}{\varphi_m^3(\hat{\boldsymbol{x}}(k), t, T)} \right. \\ \left. \frac{\left(\varphi_m^2(\hat{\boldsymbol{x}}(k), t, T) - \beta_m^2(k+t)\right)\hat{\beta}(k) + \xi_m(k+t)\beta_m(k+t)\hat{\alpha}(k)}{\varphi_m^3(\hat{\boldsymbol{x}}(k), t, T)} \right] \tag{24}$$

$$\boldsymbol{H}_m^v(k+t) = \left[\begin{array}{l} \varphi_m^2(\hat{\boldsymbol{x}}(k), t, T)\left(\alpha_m(k+t) + tT\hat{\beta}(k)\right) \\ \quad - tT\left(\alpha_m^2(k+t)\hat{\alpha}(k) + \alpha_m(k+t)\beta_m(k+t)\hat{\beta}(k)\right) \\ \hline \varphi_m^3(\hat{\boldsymbol{x}}(k), t, T) \end{array} \right., \\ \left[\frac{\varphi_m^2(\hat{\boldsymbol{x}}(k), t, T)\left(\beta_m(k+t) + tT\hat{\beta}(k)\right) - tT\left(\beta_m^2(k+t)\hat{\beta}(k) + \alpha_m(k+t)\beta_m(k+t)\hat{\alpha}(k)\right)}{\varphi_m^3(\hat{\boldsymbol{x}}(k), t, T)} \right] \tag{25}$$

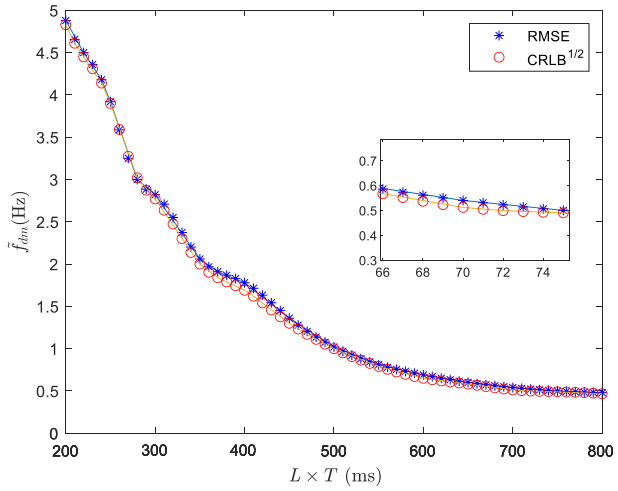

(a) Sensor #1

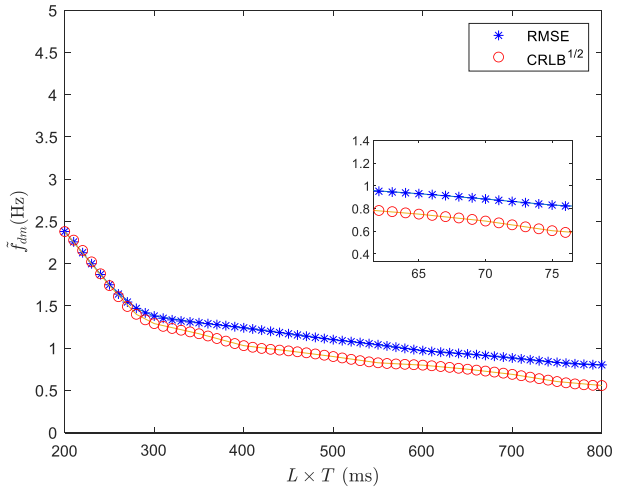

(b) Sensor #2

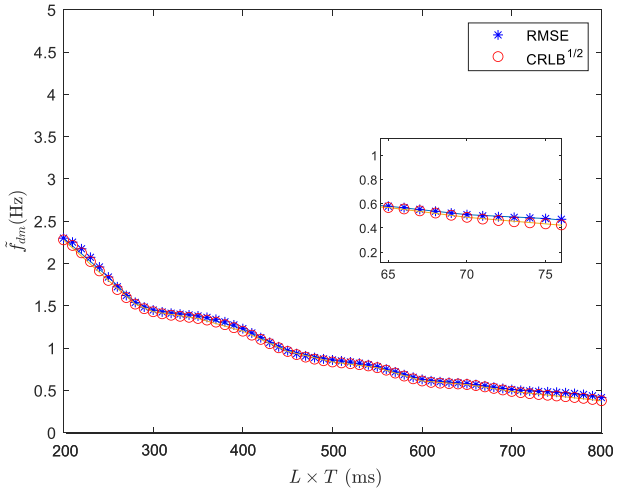

(c) Sensor #3

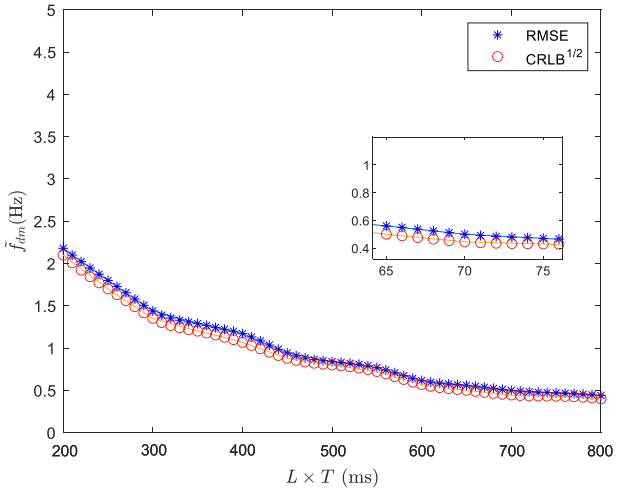

(d) Sensor #4

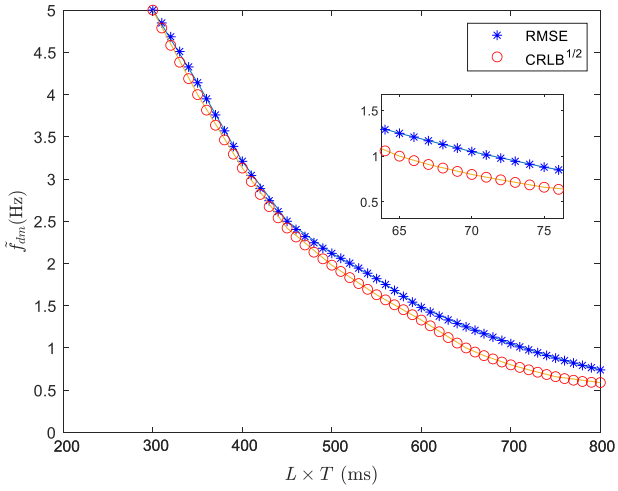

(e) Sensor #5

FIGURE 1. **Comparison of Bias estimation between RMSE and CRLB for different time windows *L* (static sensors).**

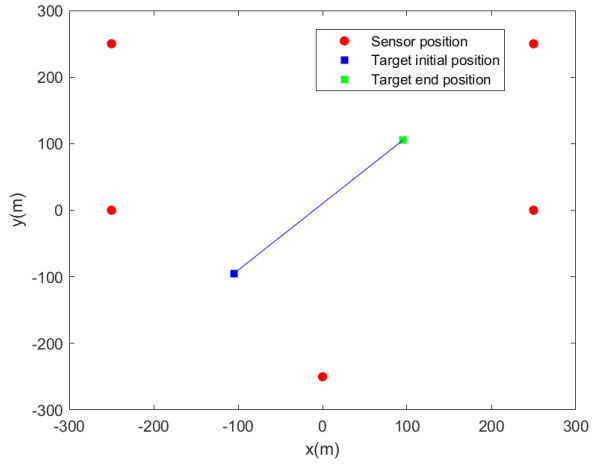

FIGURE 2. Sensor locations and target trajectory (static sensors).

where $\boldsymbol{p}$ and $\boldsymbol{v}$ represent the actual position vector and velocity vector of the target, respectively, at the initial time of the measurement window.

In order to measure the performance of the proposed algorithm more scientifically, the results of the Kalman filter are compared. Kalman filter is a classical state estimation algorithm, which is applied in various fields. However, it should be noted that this paper focuses on joint estimation, and the Kalman filter cannot solve it alone.

The number of Monte Carlo simulations is set to 100, and the root mean square error (RMSE) is used to evaluate the estimation errors of the Monte Carlo simulations.

A. STATIC DOPPLER SENSORS SCENARIO

The five Doppler sensors are symmetrically distributed in a specific two-dimensional area, with the following coordinates: [−250m, 0m], [−250m, 250m], [250m, 250m], [250m, 0m], [0m, −250m]. The simulation scenario for collaborative tracking using static Doppler sensors is illustrated in Fig. (2).

To illustrate the effectiveness of our proposed algorithm, the estimation performances of measurement bias employing different lengths L of the time window are compared, and the CRLBs are borrowed as competitors. Fig. (1) shows the RMSE of the bias estimation for each sensor. As the length of the time window L increases, the performance of the bias estimation improves. Since the time window length L represents how much data is used for estimation, such an improvement is expected.

Fig. (3) shows the RMSE of the target state estimation. JTSE (Joint Target State Estimation) represents the result of the proposed algorithm with bias-compensated. KF represents the result of Kalman filter. TSE (Target State Estimation) represents the result of the proposed algorithm with uncompensated. At the same time t, the estimation results of JTSE, KF, and TSE are compared. It is evident that both the position RMSE and velocity RMSE decrease substantially, and achieve better performance compared to KF. This demonstrates that the algorithm

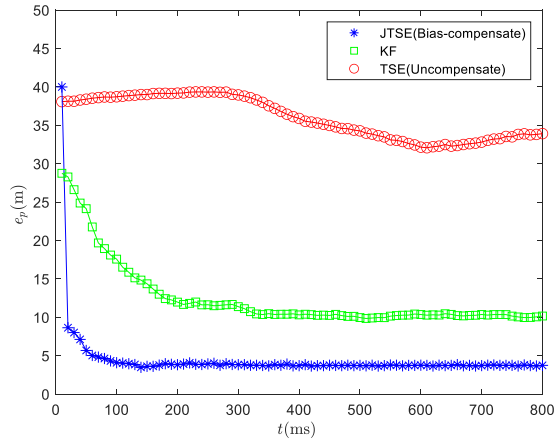

(a) Position RMSE

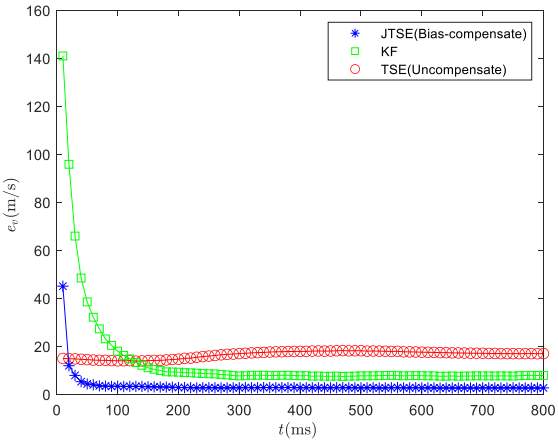

(b) Velocity RMSE

FIGURE 3. Comparison of RMSE between JTSE, KF, and TSE for different times (static sensors).

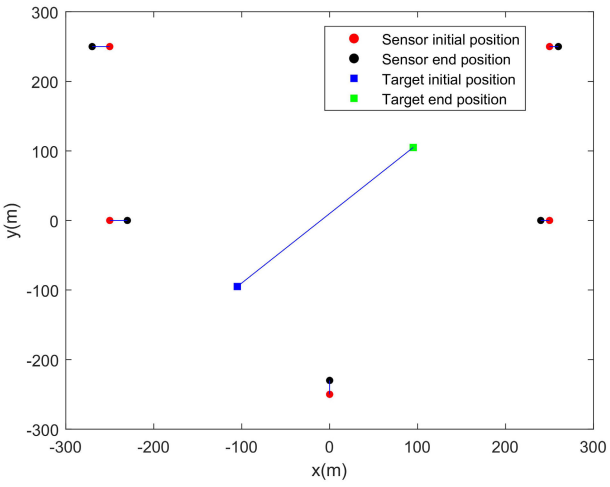

FIGURE 4. Sensor trajectories and target trajectory (moving sensors).

presented in this paper enhances the performance of the target state estimation for biased Doppler-only sensors. The e_p of final convergence is less than $5m$, and e_v is less than $3m/s$.

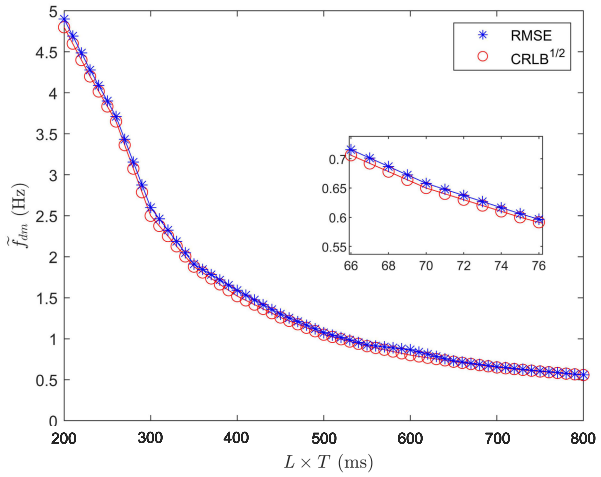

(a) Bias estimation for sensor #1 versus L

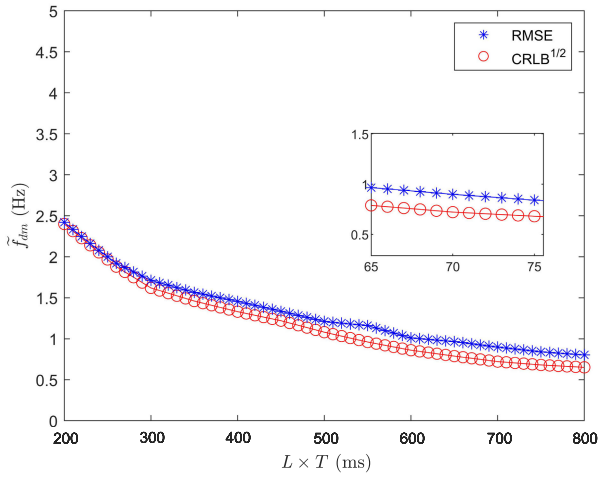

(b) Bias estimation for sensor #2 versus L

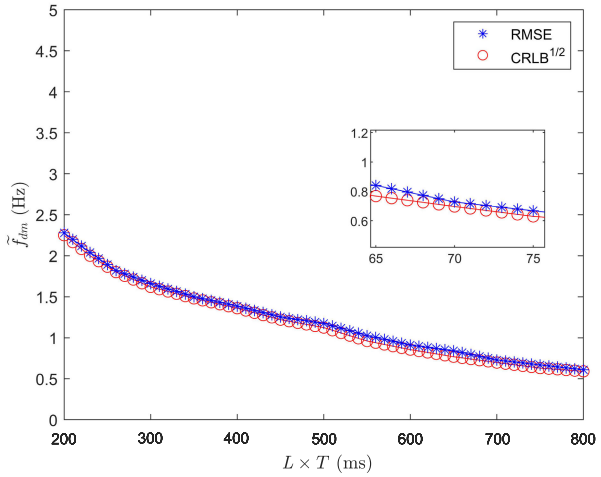

(c) Bias estimation for sensor #3 versus L

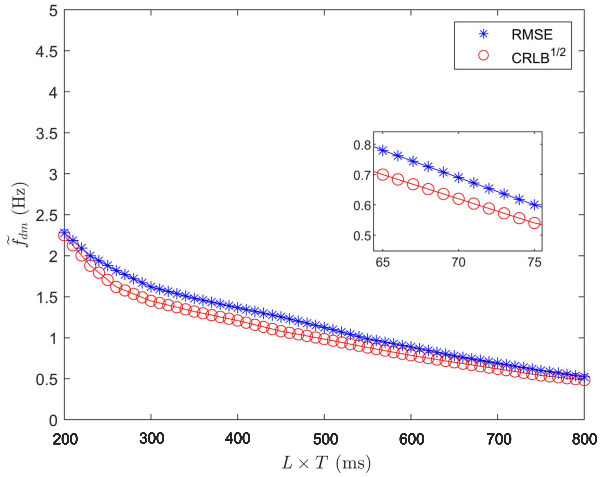

(d) Bias estimation for sensor #4 versus L

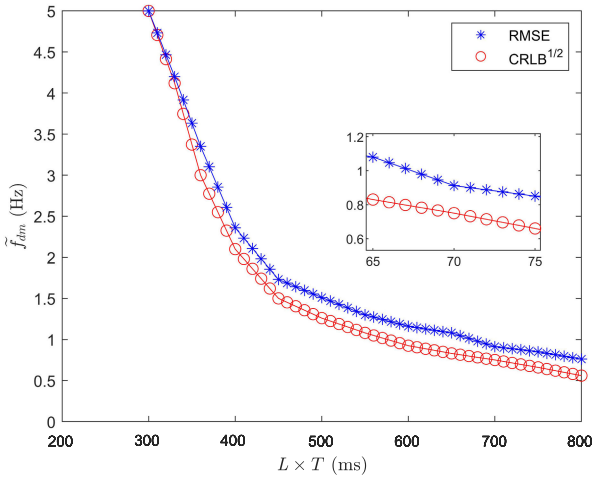

(e) Bias estimation for sensor #5 versus L

FIGURE 5. **Comparison of Bias estimation between RMSE and CRLB for different time windows L (moving sensors).**

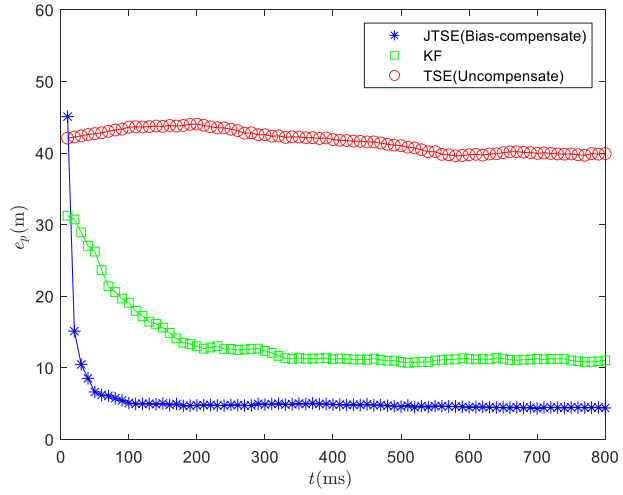

(a) Position RMSE

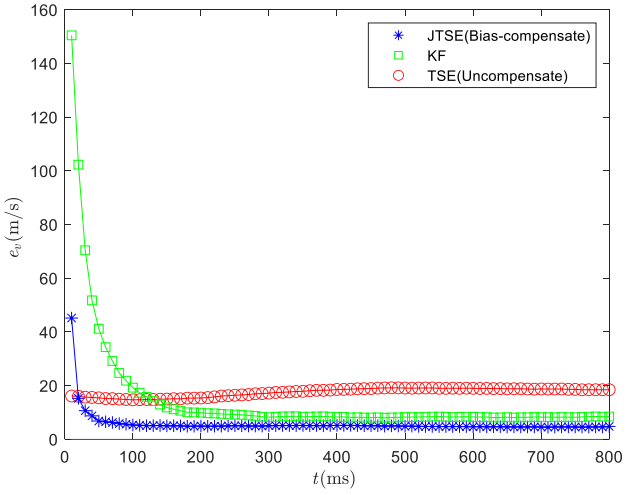

(b) Velocity RMSE

FIGURE 6. Comparison of RMSE between JTSE, KF, and TSE for different times (moving sensors).

B. MOVING DOPPLER SENSORS SCENARIO

To verify the effectiveness of our algorithm in the scenario of multiple moving Doppler sensors, additional simulations are conducted. The simulation parameters of the target motion model remain consistent with those listed in the previous subsection. The initial positions of the five Doppler sensor platforms in two-dimensional space remain the same. The states of each sensor are initialized as follows: $[-250\text{m}, 0\text{m}, 20\text{m/s}, 0\text{m/s}]^{\text{T}}$, $[-250\text{m}, 250\text{m}, -20\text{m/s}, 0\text{m/s}]^{\text{T}}$, $[250\text{m}, 250\text{m}, 10\text{m/s}, 0\text{m/s}]^{\text{T}}$, $[250\text{m}, 0\text{m}, -10\text{m/s}, 0\text{m/s}]^{\text{T}}$, $[0\text{m}, -250\text{m}, 0\text{m/s}, 20\ /\text{s}]^{\text{T}}$. The initial state of the target and the configurations of the measurement bias vector remain unchanged. The simulation scenario with moving Doppler sensors is shown in Fig. (4).

Similarly, in the scenario with moving sensor platforms, the performances of bias estimations with the CRLB under different lengths of measurement windows L are compared. The RMSE of each measurement bias estimation is illustrated in Fig. (5).

The comparison of JTSE (Bias-compensate), KF, and TSE (Uncompensate) is shown in Fig. (6). As in the previous subsection, the estimation results of the bias compensation and those of the no-bias compensation are compared. It is proven that the algorithm proposed in this paper can also significantly improve the performance of target state estimation when the Doppler-only sensors are not static.

V. CONCLUSION

A novel joint estimation algorithm for the target state and measurement bias is proposed in this study to address the problem of estimation precision for biased Doppler-only sensors. Doppler shift is used as the measurement. First, a preliminary estimation of the target state is carried out, without considering the existing measurement bias of the Doppler-only sensors. After the preliminary estimation, the measurement equation containing the measurement bias is linearized using a time window. The target state and measurement bias are obtained using the least-squares method. Moreover, the Cramer-Rao lower bound of bias estimation is investigated in this study as well. The superiority of our proposed algorithm is verified by simulations in two different scenarios, i.e., static Doppler sensors and moving Doppler sensors. Simulation results show that compared with other state estimation algorithms without measurement bias compensating, e.g., Kalman filter, the performance of both position and velocity RMSE of our algorithm is better. In different scenarios, the position RMSE can be reduced by 6m, and the velocity RMSE can be reduced by 5m/s. Future work might lie in the following potential directions: using the proposed algorithm in three-dimensional scenarios, developing algorithms that can obtain the joint estimation of the target state and measurement bias recursively based on approaches such as the Kalman filter, and expanding our algorithm to the scenarios in which there are multiple maneuvering targets.

APPENDIX A ABBREVIATIONS

The following abbreviations are used in this manuscript:

MIMO	Multiple Input Multiple Output
TOA	Time of Arrival
DOA	Direction of Arrival
KF	Kalman Filter
JTSE	Joint Target State Estimation
TSE	Target State Estimation
FIM	Fisher Information Matrix
CV	Constant Velocity
CRLB	Cramer-Rao Lower Bound
RMSE	Root Mean Square Error

APPENDIX B
ALGORITHM 1

Algorithm 1 Joint Estimation Algorithm of Target State and Measurement Bias

Input: $z_k, \ldots, z_{k+L-1}, s_1, \ldots, s_M, \lambda, M, L, k$;

Output: $\hat{p}_k, \hat{v}_k, \hat{f}_{d1}, \ldots, \hat{f}_{dM}$;

for all $i = k, k+1, \cdots, k+L-1$ **do**

$\boldsymbol{P}_A(\boldsymbol{p}_k) = \mathbf{I} - \boldsymbol{A}(\boldsymbol{p}_k)\left(\boldsymbol{A}^{\mathrm{T}}(\boldsymbol{p}_k)\boldsymbol{A}(\boldsymbol{p}_k)\right)^{-1}\boldsymbol{A}^{\mathrm{T}}(\boldsymbol{p}_k)$.

$\hat{\boldsymbol{p}}_k = \arg\min_{\boldsymbol{p}_k} \boldsymbol{\eta}_k^{\mathrm{T}} \boldsymbol{P}_A(\boldsymbol{p}_k)\boldsymbol{\eta}_k$

$\hat{\boldsymbol{v}}_k = \left(\boldsymbol{A}^{\mathrm{T}}(\hat{\boldsymbol{p}}_k)\boldsymbol{A}(\hat{\boldsymbol{p}}_k)\right)^{-1}\boldsymbol{A}^{\mathrm{T}}(\hat{\boldsymbol{p}}_k)\boldsymbol{\eta}_k$.

Construct $\boldsymbol{C}_i, \boldsymbol{d}_i$ according to (29)-(32);

end for

$\boldsymbol{C} = [\boldsymbol{C}_k; \boldsymbol{C}_{k+1}; \cdots; \boldsymbol{C}_{k+L-1}]$

$\boldsymbol{d} = [\boldsymbol{d}_k; \boldsymbol{d}_{k+1}; \cdots; \boldsymbol{d}_{k+L-1}]$

$\hat{\boldsymbol{\theta}} = \left(\boldsymbol{C}^{\mathrm{T}}\boldsymbol{C}\right)^{-1}\boldsymbol{C}^{\mathrm{T}}\boldsymbol{d}$

$\hat{\boldsymbol{p}}_k = \hat{\boldsymbol{p}}_k + \hat{\boldsymbol{\theta}}(1:2)$,

$\hat{\boldsymbol{v}}_k = \hat{\boldsymbol{v}}_k + \hat{\boldsymbol{\theta}}(3:4)$,

$\hat{f}_{d1}, \ldots, \hat{f}_{dM} = \hat{\boldsymbol{\theta}}(5:M+4)$

return $\hat{\boldsymbol{p}}_k, \hat{\boldsymbol{v}}_k, \hat{f}_{d1}, \ldots, \hat{f}_{dM}$.

REFERENCES

[1] J. Y. Zhang, K. Dong, and S. Sun, "Target tracking algorithm of Doppler radar based on CKF," *Ship Electron. Eng.*, vol. 41, pp. 51–57, Dec. 2021.
[2] H. D. Wang, D. Kai, Y. S. Zhi, and F. Qiang, "Multi-target joint detection and estimation of Doppler radar based on superpositional sensors," *J. Signal Process.*, vol. 38, pp. 964–972, May 2022.
[3] W. Dong, J. Wang, Z. Song, and Q. Fu, "A joint detection and state estimation algorithm for pulse Doppler radar," in *Proc. IEEE 5th Inf. Technol., Netw., Electron. Autom. Control Conf. (ITNEC)*, Oct. 2021, pp. 345–353.
[4] S. Burintramart, T. K. Sarkar, Y. Zhang, and M. Salazar-Palma, "Nonconventional least squares optimization for DOA estimation," *IEEE Trans. Antennas Propag.*, vol. 55, no. 3, pp. 707–714, Mar. 2007.
[5] K. Zhu, Y. Wei, and R. Xu, "TOA-based localization error modeling of distributed MIMO radar for positioning accuracy enhancement," in *Proc. CIE Int. Conf. Radar (RADAR)*, Oct. 2016, pp. 1–5.
[6] S. T. Goh, S. A. Zekavat, and K. Pahlavan, "DOA-based endoscopy capsule localization and orientation estimation via unscented Kalman filter," *IEEE Sensors J.*, vol. 14, no. 11, pp. 3819–3829, Nov. 2014.
[7] A. R. Nafchi, S. T. Goh, and S. A. R. Zekavat, "High performance DOA/TOA-based endoscopy capsule localization and tracking via 2D circular arrays and inertial measurement unit," in *Proc. IEEE Int. Conf. Wireless Space Extreme Environ.*, Nov. 2013, pp. 1–6.
[8] V. Karaev, Y. Titchenko, M. Panfilova, M. Ryabkova, E. Meshkov, and K. Ponur, "Application of the Doppler spectrum of the backscattering microwave signal for monitoring of ice cover: A theoretical view," *Remote Sens.*, vol. 14, no. 10, p. 2331, May 2022.
[9] X. Zhou, H. Ma, and H. Xu, "An experimental multi-target tracking of AM radio-based passive bistatic radar system via multi-static Doppler shifts," *Sensors*, vol. 21, no. 18, p. 6196, Sep. 2021.
[10] L. R. Malling, "Radio Doppler effect for aircraft speed measurements," *Proc. IRE*, vol. 35, no. 11, pp. 1357–1360, Nov. 1947.
[11] S. Salinger and J. Brandstatter, "Application of recursive estimation and Kalman filtering to Doppler tracking," *IEEE Trans. Aerosp. Electron. Syst.*, vol. AES-6, no. 4, pp. 585–592, Jul. 1970.
[12] S. Kim, D. Oh, and J. Lee, "Joint DFT-ESPRIT estimation for TOA and DOA in vehicle FMCW radars," *IEEE Antennas Wireless Propag. Lett.*, vol. 14, pp. 1710–1713, 2015.
[13] E. Taghavi, R. Tharmarasa, T. Kirubarajan, and M. Mcdonald, "Multisensor-multitarget bearing-only sensor registration," *IEEE Trans. Aerosp. Electron. Syst.*, vol. 52, no. 4, pp. 1654–1666, Aug. 2016.
[14] Y.-C. Xiao, P. Wei, and T. Yuan, "Observability and performance analysis of bi/multi-static Doppler-only radar," *IEEE Trans. Aerosp. Electron. Syst.*, vol. 46, no. 4, pp. 1654–1667, Oct. 2010.
[15] M. Lesturgie and D. Poullin, "Frequency allocation in radar: Solutions and compromise for low frequency band," in *Proc. 5th Int. Conf. Exhib. Radar Syst.*, Brest, France, 1999.
[16] A. Martone and M. Amin, "A view on radar and communication systems coexistence and dual functionality in the era of spectrum sensing," *Digit. Signal Process.*, vol. 119, Dec. 2021, Art. no. 103135.
[17] S. Ayazgök and U. Orguner, "Optimal sensor placement for Doppler-only target tracking: 1D target motion case," in *Proc. 19th Int. Conf. Inf. Fusion (FUSION)*, Jul. 2016, pp. 2283–2288.
[18] C. Chai, T. Yang, and N. Lyu, "Roadside multi-sensor data fusion based on adaptive federal Kalman filtering," in *Proc. 7th Int. Conf. Transp. Inf. Saf. (ICTIS)*, Xi'an, China, Aug. 2023, pp. 744–751.
[19] C. He, M. Zhang, and F. Guo, "Bias compensation for AOA-geolocation of known altitude target using single satellite," *IEEE Access*, vol. 7, pp. 54295–54304, 2019.
[20] G. Fukuda and N. Kubo, "Application of initial bias estimation method for inertial navigation system (INS)/Doppler velocity log (DVL) and INS/DVL/gyrocompass using micro-electro-mechanical system sensors," *Sensors*, vol. 22, no. 14, p. 5334, Jul. 2022.
[21] J. K. Y. Goh and R. Yang, "Doppler bearing tracking with fusion from heterogeneous passive sensors: ESM/EO and acoustic," in *Proc. 22th Int. Conf. Inf. Fusion (FUSION)*, Jul. 2019, pp. 1–8.
[22] Y.-C. Xiao, P. Wei, and T. Yuan, "Doppler frequency-only and T2/R radar based moving target location," in *Proc. CIE Int. Conf. Radar*, Oct. 2006, pp. 1–4.

GUOQIANG SUN received the B.S. degree in automation from the Dalian University of Technology, in 2022. He is currently pursuing the M.S. degree with Xi'an Jiaotong University. His current research interests include information fusion, target tracking, and threat assessment.

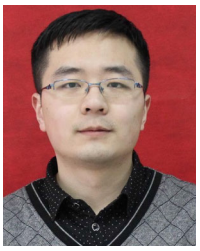

TAO YAN received the B.S. degree in control science and engineering and the Ph.D. degree in control theory and control engineering from the Faculty of Electronic and Information Engineering, Xi'an Jiaotong University, Xi'an, China, in 2007 and 2014, respectively.

He has been a member of the Faculty of Electronic and Information Engineering, Xi'an Jiaotong University, since 2015, where he is currently a member and an Associate Professor with the Ministry of Education Key Laboratory for Intelligent Network and Network Security and the School of Automation. From 2009 to 2011, he did research on target classification with the Department of Electrical and Computer Engineering, University of Calgary, Calgary, AB, Canada. His research interests include information fusion, target tracking, sensor management, rough set theory, data mining, and knowledge discovery.

ZIXIONG YANG received the B.S. degree in electrical engineering and automation from Wuhan University, in 2020. He is currently pursuing the M.S. degree in automation with Xi'an Jiaotong University. His current research interests include information fusion, passive target tracking, and sensor management.

WENBO WU received the B.S. degree in automation from Xi'an Jiaotong University, in 2023, where he is currently pursuing the M.S. degree. His current research interests include information fusion, sensor management, and target tracking.